Published in final edited form as:
Neuroimage. 2012 September ; 62(3): 1726–1731. doi:10.1016/j.neuroimage.2012.05.010.

Contrast-Enhanced Functional Blood Volume Imaging (CE-fBVI): Enhanced Sensitivity for Brain Activation in Humans using the Ultrasmall Superparamagnetic Iron Oxide Agent Ferumoxytol

Deqiang Qiu[1], **Greg Zaharchuk**[1], **Thomas Christen**[1], **Wendy W Ni**[1,2], and **Michael E Moseley**[1]

[1]Department of Radiology, Stanford University, CA, USA

[2]Department of Electrical Engineering, Stanford University, CA, USA

Abstract

Functional MRI (fMRI) brain studies performed in the presence of a steady-state or "blood pool" contrast agent yields activation maps that are weighted for cerebral blood volume (CBV). Previous animal experiments suggest significant contrast-to-noise (CNR) improvements, but these studies have not yet been performed in humans due to the lack of availability of a suitable agent. Here we report the use of the USPIO ferumoxytol (AMAG Pharmaceuticals, Inc., Cambridge, MA) for functional brain activation in humans, termed contrast enhanced functional Blood Volume Imaging (CE-fBVI). Four subjects were scanned during a unilateral finger tapping task with standard blood-oxygen level dependent (BOLD) imaging before contrast and CE-fBVI after contrast injection. The CE-fBVI response showed both a fast (5.8±1.3 sec) and a slow (75.3±27.5 sec) component of CBV response to stimuli. A significant CNR gain of approximately 2–3 was found for CE-fBVI compared to BOLD fMRI. Interestingly, less susceptibility-related signal dropouts were observed in the inferior frontal and temporal lobes with CE-fBVI. The combination of higher CNR and better spatial specificity, enabled by CE-fBVI using blood pool USPIO contrast agent opens the door to higher resolution brain mapping.

Keywords

fMRI; contrast agents; USPIO; human; brain activation; MRI; blood-pool

Introduction

Functional MRI using blood oxygenation level dependent (BOLD) has allowed the study of physiological and neural processes in response to external stimuli (Ogawa et al., 1990; Ogawa et al., 1993). The BOLD signal depends on complex and dynamic interactions between cerebral vascular responses to neural activation, including cerebral blood flow (CBF), cerebral blood volume (CBV), and oxygenation (Buxton et al., 1998; Lin et al., 2008; Malonek and Grinvald, 1996). Ultrasmall superparamagnetic iron oxide (USPIO)

Corresponding Author: Deqiang Qiu, PhD (qiudeqiang@gmail.com) or Michael E. Moseley, PhD (moseley@stanford.edu) Lucas Center for MR imaging, MC 5488, 1201 Welch Road, Stanford, CA 94305-5488, USA, Tel: +1 650 725-6077, FAX: +1 650 723-9222.

agents provide a strong T2* MR contrast mechanism which alters MR signal in relation to CBV (Boxerman et al., 1995; Weisskoff et al., 1994). Because of its small diameter, USPIO particles are not rapidly cleared by the reticuloendothelial system and, therefore, have long blood plasma half-lives (Weinstein et al., 2010). The presence of USPIO causes signal reduction that is dependent on CBV, which changes during neuronal activation (Belliveau et al., 1991). Therefore, MR signal changes in the presence of USPIO primarily reflect dynamics of CBV during neural activity, which overwhelms the signal changes due to deoxyhemoglobin concentration changes (Leite et al., 2002; Lu et al., 2007; Mandeville et al., 2004; Mandeville et al., 1998). Such CBV-based methods also facilitate comparison between subjects and different centers, as signal changes can be directly translated to changes of physiological parameters (Mandeville et al., 2004). Leite et al (Leite et al., 2002) used USPIO in macaques and showed dramatically improved activation sensitivity using USPIO-based fMRI compared to BOLD fMRI. Furthermore, unlike BOLD fMRI which has relatively low spatial specificity due to sensitivity to large vessels, CBV based fMRI was found to provide high spatial specificity allowing study of the ocular dominance field in animal models (Harel et al., 2006; Zhao et al., 2006).

The advantages of high detection sensitivity and spatial specificity make CBV-based fMRI using USPIO particles as exogenous contrast agents an appealing technique for human studies. Until now, there has been no human study on the use of USPIO for CBV based fMRI, or what we term contrast-enhanced functional blood volume imaging (CE-fBVI). In the current work, we explore the feasibility of CBV based fMRI in humans using ferumoxytol, an USPIO that is FDA-approved for treatment of iron deficiency anemia in adult patients with chronic kidney disease. Specifically, we studied the time constants of the CBV response to neural activity and the contrast-to-noise ratio (CNR) gain of CE-fBVI over BOLD fMRI. We hypothesized that significantly higher CNR can be obtained for CE-fBVI compared to BOLD.

Theory

The presence of USPIO causes a linear R2* change as a function of concentration (Boxerman et al., 1995; Mandeville et al., 1998).

$$\Delta R_2^* = K \cdot CBV \quad [1]$$

where K is a function of the concentration of contrast agent. Following the derivation of (Mandeville et al., 1998) and (Lu et al., 2007), the relaxation coefficient $R2^{*,\,\mathrm{post}}$ at resting state after the contrast injection is

$$R_2^{*,post} = R_2^{*,pre} + K \cdot CBV_0 \quad [2]$$

where $R_2^{*,\,\mathrm{pre}}$ is the relaxation coefficient at resting state before contrast injection, and CBV_0 is the cerebral blood volume at resting state. The signal intensity at resting state after contrast injection is

$$S_{post,base} = S_0 \cdot \exp(-TE \cdot R_2^{*,post}) \quad [3]$$

The signal intensity during neural activation is:

$$S(t) = S_{post,base} \exp(-TE \cdot K \cdot \Delta CBV(t)) \cdot \exp(-TE \cdot \Delta R_2^{*,BOLD}(t)) \quad [4]$$

And the change in signal intensity with respect to resting state is then:

$$\Delta S(t)=S(t)-S_{post,base}\approx -S_0\cdot\exp(-TE\cdot R_2^{*,post})\cdot TE\cdot(K\cdot\Delta CBV(t)+\Delta R_2^{*,BOLD}(t)) \quad [5]$$

The approximation in the second derivation gives close estimate when the change is small, and the error is about 4% for a true change of 25%.

Here, S_0 is signal intensity at TE=0. R_2 *, pre and R_2 *, post are transverse relaxation constant before and after contrast injection respectively; ΔCBV(t) change in CBV; ΔR_2*, BOLD, change in transverse due to BOLD effect.

When TE is fixed, the maximum signal change is achieved at a contrast concentration when

$$K=\frac{1}{TE\cdot CBV_0}-\frac{\Delta R_2^{*,BOLD}}{\Delta CBV} \quad [6]$$

When the contrast concentration, i.e. K is fixed, the maximum signal change is achieved when:

$$TE=\frac{1}{R_2^{*,post}} \quad [7]$$

For subjects scanned with the same with same TE for both BOLD and CE-fBVI, the percentage CBV change during task can be calculated as:

$$\frac{\Delta CBV}{CBV_0}=\frac{\log(S_{post,act}/S_{pre,act})}{\log(S_{post,base}/S_{pre,base})}-1, \quad [7]$$

where $S_{pre,\,act}$ and $S_{post,\,act}$ are signal intensities during BOLD and CE-fBVI task respectively, and $S_{pre,\,base}$ and $S_{post,\,base}$ are signal intensities at resting state before and after contrast injection respectively.

It is important to notice that the detection sensitivity also depends on noise, and the temporal noise in fMRI data include three components (Kruger and Glover, 2001): $\sigma=\sqrt{\sigma_0^2+\sigma_B^2+\sigma_{NB}^2}$, where σ_0 is the thermal and system noise that is independent of signal and is expected to be unchanged before and after contrast injection. σ_B and σ_{NB} represent physiological noises that arise from baseline fluctuations in cerebral blood flow, cerebral blood volume and cerebral blood oxygenation level as well as cardiac and respiratory functions. σ_B represents the component that results in fluctuation in R_2^*. This component is closed related to spontaneous brain activity at resting state through the same mechanism of tasked induced responses as well as cardiac and respiratory functions. This component is proportional to contrast changes in BOLD experiments. σ_{NB} represents physiological noise that is independent of TE but is proportional to the signal intensity.

Methods

Subjects

Four healthy right-handed male volunteers were recruited for the study (24 years to 53 years old). This research was approved by the institutional review board and informed consent was obtained from each volunteer.

Data Acquisition

MR imaging was performed at 3T with an 8-channel head coil (MR750, GE Healthcare, Waukesha, WI). Subjects were scanned with the following protocol: A 3D T1-weighted inversion recovery spoiled gradient echo (IR-SPGR) sequence covering the entire brain was acquired (TR/TE/TI = 9.2/3.7/400ms, Matrix = 256×206, in-plane resolution = 0.94 × 0.94 mm, slice thickness = 1.2mm, 120–130 slices depending on head size). BOLD fMRI and CE-fBVI were performed using a 2D gradient echo EPI sequence before and after the slow injection (1ml/s) of ferumoxytol (510 mg Fe [approx 7 mg Fe/kg], AMAG Pharmaceuticals, Cambridge, MA) respectively (FOV=22cm, Matrix = 64×64, slice thickness = 4 mm, number of slices = 36, TR=2s). The subjects performed 4 epochs of 48s of right hand finger tapping and 48s of rest in response to auditory cues. The echo time (TE) was 35ms for pre-contrast BOLD. To experimentally validate the optimal TE for CE-fBVI, one subject underwent CE-fBVI scans with both 20ms and 35ms, another one with TE of 20ms, and the other two subjects with TE of 35ms. A 3D multi-echo gradient echo sequence was acquired for T2* mapping before and after contrast injection (16 echoes with a smallest TE of 3.3ms and an echospacing of 4ms, Matrix = 256×232, in-plane resolution = 0.86 × 0.86mm, 10 slices of 1mm thick).

$T2^*$ calculation

Images were processed using SPM8 (Wellcome Trust Center of Neuroimaging, UCL, UK) and custom MATLAB (Mathwork, Natick MA) scripts. T2* maps were generated by fitting the following formula using Levenberg-Marquardt algorithm

$$S(TE)=S0\cdot\exp(-TE/T2*)+\sigma \quad [8]$$

where S(TE) is the signal at echo time of TE, σ is the noise level which was measured in the image at a region of air. The noise term σ was added to the model because at long echo time after contrast injection the signal approaches noise floor. The 3D T1-weighted image was segmented using SPM8 and re-sliced to the space of the T2* map. A gray matter mask was then created and used to calculate the mean T2* value of the gray matter before and after contrast injection.

fMRI Image Analysis

The 2D gradient EPI images from both BOLD and CE-fBVI experiments were first co-registered to correct for motion and then smoothed with a Gaussian kernel with a full-width half height of 7mm. A general linear model was used for the detection of activated region, where a hemo-response function (HRF) was convolved with the paradigm as a regressor. For BOLD fMRI, the canonical HRF from SPM8 was used, while for CE-fBVI the HRF was generated with the bi-exponential model fit described below. The activated region in the motor area was identified from BOLD fMRI and a region of 3×3×3 voxels from the unsmoothed images was exacted. The mean value in this area was used to estimate the time constants of both BOLD and CBV responses by fitting mono- or bi-exponential model with the following equation using Levenberg-Marquardt algorithm:

$$R(t)=\sum_{i=1}^{n} a_i \cdot \exp(-Tc_i \cdot t) \quad [9]$$

where n = 1 for mono-exponential model, and n= 2 for bi-exponential model; Tc_i characterizes the response speed of the BOLD or CE-fBVI to external stimuli; a_i specifies the relative weighting the of the two exponential terms in the bi-exponential model and $a_1+a_2 = 1$.

The relative sensitivity of BOLD fMRI and CE-fBVI were compared using CNR ratio and Student's T statistics. We define the contrast to noise ratio (CNR) to be the ratio between the standard deviation of fitted signal time course and σ_0, It is defined against σ_0 instead of σ so that CNR does not depends on image resolution, which affects signal intensity and hence σ. The standard deviation of the fitted signal time course quantifies the amount of variance in the data that is explained by the fit, which is consistent with the definition of commonly used F statistics in linear regression. To quantify the number of voxels activated in the primary motor cortex, a mask image of the primary motor cortex was generated in the MNI (Montreal Neurological Institute) space and then dilated by 2cm to account for subject variability. The MNI T1 weighted image was then registered to the mean EPI image of each subject, and the transformation derived was then applied to the dilated primary motor cortex mask to create masks in image space of individual subjects. The peak t value (T_{peak}), average t value in the commonly activated region (T_{cn}), and average t value of the 50 most activated voxels in the respective method (T_{50}) were quantified for both BOLD and CE-fBVI.

To quantify the temporal noise of BOLD and CE-fBVI, the mean and temporal standard deviation of first 24 time points (48s) when the subject was resting for both BOLD and CE-fBVI. The T1 weighted image was segmented using SPM and a gray matter mask was created and registered to the image space of BOLD and CE-fBVI. Then mask was then used to calculate the mean signal intensity (S_{GM}) and mean temporal standard deviation in gray matter (SD_{GM}) for BOLD and CE-fBVI.

Analysis of Signal Dropout

We also compared the level of signal dropout between BOLD and CE-fBVI in the frontal region due to susceptibility difference at the air-tissue interface. A region of interest (ROI) was placed in the frontal region where signal dropout was observed, and a control ROI was placed in a posterior region of the brain. Signal dropout ratio was calculated as the ratio of the mean signal intensities between the two regions.

Results

Figure 1 shows T2*-weighted and T2* maps acquired before and 5–10 minutes after contrast injection. Significant signal decreases after contrast injection were observed due to the strong T2* effect of ferumoxytol, more so in gray matter than in white matter. The mean(SD) T2* value of the gray matter was 50.8(2.0) ms and 23.2(1.9) ms before and after contrast injection respectively (Table 1).

Robust activation was observed for both BOLD and CE-fBVI, in regions including primary and supplemental motor regions, and the cerebellum (Figure 2). Generally, at the resolution acquired in the present study, activated regions overlapped between CE-fBVI and BOLD, although this overlap was not perfect. For example, in one subject, there was a large activated region in the occipital lobe with CE-fBVI, which was not seen in the BOLD activation maps. The overlap between of activated CE-fBVI and BOLD in the primary motor cortex was 67.6% (3.5%) and 55.0% (21.9%) for subjects with TE=20ms and

TE=35ms respectively. Figure 3 shows an example of the signal time course during BOLD and CE-fBVI acquisition. The BOLD effect induced a positive signal change during the task with respect to resting state, with a relatively short time constant (Table 2); therefore, the signal plateaued after short period time of task and it returned to the baseline during rest. In contrast, CE-fBVI induced signal reduction during the task due to increased CBV; the time constant was longer than BOLD and the signal did not return to baseline during rest. A mono-exponential model provided a reasonable fit to the BOLD response with time constant ranging from 3.8s to 8s (Table 2). As the mono-exponential model did not provide a sufficient fit for the CE-fBVI response, particularly lack of fit for baseline, a bi-exponential model was explored. The adjusted R^2, which penalizes the number of parameter in the model against goodness of the fit the model, suggested a bi-exponential model was better than a mono-exponential model for fitting the CE-fBVI signal response. A fast and a slow component of the CE-fBVI response were observed. The response time for the faster component ranged from 3.9s to 7.0s, which was close to the response time of BOLD. The relative weighting of the fast component ranged from 0.83 to 0.92. The response time of the slower component ranged from 48.2s to 115.2s. For subjects scanned with same TE=35ms for both BOLD and CE-fBVI, the mean (SD) percentage peak CBV change was found to be 26.1%(8.7%) during task.

The CNR gain of CE-fBVI at TE=20ms was 2.0 and 2.9 for the two subjects evaluated with these parameters, respectively. For CE-fBVI at TE=35ms, the gain was 1.1, 1.5 and 2.0 for three of the subjects. Higher t statistics was obtained for CE-fBVI compared to BOLD (Figure 2). Table 3 shows peak T (T_{peak}), average T value in the 50 most significant voxels in the primary motor cortex (T_{50}), average T value in regions commonly activated in both BOLD and CE-fBVI, the mean signal intensity of gray matter (S_{GM}) and temporal standard deviation of signal in gray matter (SD_{GM}). A sensitivity gain of a factor of 1.6 in both T_{peak} and T_{50} were observed for CE-fBVI with TE=20ms over BOLD, and the factor was 1.4 and 1.3 for T_{peak} and T_{50} respectively for CE-fBVI with TE=35ms. The mean signal intensity of gray matter, S_{GM} in CE-fBVI was lower than in BOLD, and the temporal variation of signal as shown by SD_{GM} was smaller though comparable in CE-fBVI compared to BOLD.

Severe signal dropout was observed for BOLD images at the frontal and basal temporal regions near air-tissue interface, which was significantly alleviated with CE-fBVI (Figure 4). The dropout ratio, defined as the ratio of signal intensity between ROIs in a frontal region and a reference region in posterior part of the brain, was calculated. For subjects scanned with CE-fBVI with TE=20ms, the mean (SD) ratio was 0.11 (0.04) and 0.36 (0.12) for BOLD and CE-fBVI, respectively. For subjects scanned with CE-fBVI with TE=35ms, the mean (SD) ratio was 0.10 (0.04) and 0.20 (0.08) for BOLD and CE-fBVI, respectively. The ratio was higher in all CE-fBVI scans with TE=35ms than their respective BOLD scans.

Discussion

To our knowledge, this is the first study that uses blood pool USPIO for functional brain activation in humans. We characterized the response time for CBV changes during neural activation, and CE-fBVI was found to have up to about a factor of 3 sensitivity gain over BOLD at the dose of 7mg Fe/kg.

CE-fBVI using USPIO primarily reflects CBV changes during neural activation, through its R_2* effect in the presence of a blood pool (persistent) contrast agent. Although it has been known that gradient echo images are sensitive to large vessels (Boxerman et al., 1995), previous studies have established that only capillaries, smaller arterioles, and some of the smallest venules are capable of constriction and dilation (Atkinson et al., 1990; Duelli and Kuschinsky, 1993; Lu et al., 2003). Therefore, CE-fBVI is more specific to changes in

microvasculature, hence providing better spatial localization. In contrast, BOLD is more sensitive to larger vessels since deoxyhemoglobin concentration is also altered in veins draining the region of neural activation. Animal studies have demonstrated the higher spatial specificity of CE-fBVI, and have shown that columnar and laminar imaging is feasible with CE-fBVI (Harel et al., 2006; Lu et al., 2004; Zhao et al., 2006).

The percentage CBV change was found to be 26.1% (8.7%), which is consistent with previous reports (Belliveau et al., 1991). We also found a fast and a slow component of the CBV response to stimuli, consistent with previous animal and human studies (Leite et al., 2002; Lu et al., 2003). It is noteworthy of the relative large inter-subject variation in the estimated time constant of the slow component of the response, which is likely the combination of true inter-subject variation and errors in the model fitting. Scanner drifts may also contribute to errors in the estimation; however signal response of BOLD did not show the similar cumulative effects of slow component observed in CE-fBVI, suggesting scanner drift is not a dominant factor in the estimation error. Larger scale studies may further characterize these variations. The fast components may reflect arteriolar and capillary components, while the slower component may represent venular contribution, which is believed to the source of the post-stimulus undershoot in the BOLD signal (Buxton et al., 1998). In a previous study of non-human primates (Leite et al., 2002), the time constant of the slower component was found to be around 14.5s and the signal level returned to baseline after 60s of resting. However, in our study, the estimated time constant of the slower component ranged from 48.2s to 115.4s, and the significant signal change was still present after 48s of rest. Shorter time constants have been observed in rodent studies (Lu et al., 2007). This suggests more prolonged venular responses in humans compared to animals.

We observed a CNR gain of CE-fBVI at 20ms over BOLD with a factor of 2.0 to 2.9. It is noteworthy that the optimal TE (~50ms) was not used for BOLD experiment. However, the CNR reduction using TE=35ms with respect to TE=50 is less than 5%. Therefore, the CNR gain is primarily due to the use of the contrast agent. This CNR gain is translated to higher t-statistics in the activation map. Comparable noise levels were also observed between CE-fBVI and BOLD. As the signal intensity is lower in CE-fBVI, it is expected that noise due to cardiac and respiratory functions and subject motion would decrease (Kruger and Glover, 2001). The finding of comparable noise levels between CE-fBVI and BOLD suggests an expected increase in noise related to intrinsic fluctuations in neural activity at resting state. However, whether this increase is proportional to CNR gain of response to external stimuli is a subject of further study, since the slower response of CBV with respect to BOLD acts as a different low-pass filter of the resting state neural activity. We observed a T statistics gain that is not proportional to CNR gain. This may be due to variations in response that is not captured by exponential model, and a larger cohort would allow the derivation of population wise canonical CBV response function that is not captured by exponential models. Together, the increased contrast sensitivity can be efficiently invested in imaging at higher image resolution.(Kruger and Glover, 2001; Triantafyllou et al., 2005). Combining the improved spatial specificity and sensitivity of CE-fBVI, it may be feasible for more accurate surgical planning and high resolution mapping of human brain functions such as orientation column mapping, which is only currently feasible using spin echo technique at 7T (Yacoub et al., 2008).

Largely overlapping regions were found activated with both CE-fBVI and BOLD. For the subject showed in Figure 2, CE-fBVI however showed a large activated region in the occipital lobe, which was not found with BOLD. This finding may be specific to the subject due to unreported visual related activities. This may also be due to the fact that CE-fBVI and BOLD have different hemodynamic responses to stimuli and that CE-fBVI has higher

sensitivity in detecting activation. Future studies with high-resolution fMRI may reveal differences in activation loci between CE-fBVI and BOLD.

We also observed less signal dropout in the inferior frontal and temporal lobes due to susceptibility variation at the air-tissue interface. We believe the reason for this is two-fold: firstly, the optimal TE is smaller with CE-fBVI than BOLD; secondly, the high susceptibility value of USPIO also partially offsets the diamagnetic effect of the brain parenchyma, leading to closer magnetic susceptibility value between the post-contrast brain and the air. The shorter TE used with CE-fBVI also allows higher temporal resolution or larger volume coverage.

In conclusion, we demonstrated the first use of USPIO for functional blood volume imaging in humans with a CNR gains of 2–3 fold compared to BOLD fMRI. Both a fast and a slow component of blood volume response were observed, and optimal CNR gain can be obtained with long stimuli. Less susceptibility-related signal dropouts were observed in the inferior frontal and temporal lobes with CE-fBVI. The combination of CE-fBVI using blood pool contrast agents opens the door for improved human brain mapping.

Acknowledgments

The study was supported by National Institute of Health (2RO1NS047607, 1R01NS066506, 5P41RR09784), GE Healthcare, Lucas Foundation and Oak Foundation.

References

Atkinson JL, Anderson RE, Sundt TM Jr. The effect of carbon dioxide on the diameter of brain capillaries. Brain Res. 1990; 517:333–340. [PubMed: 2115812]

Belliveau JW, Kennedy DN Jr, McKinstry RC, Buchbinder BR, Weisskoff RM, Cohen MS, Vevea JM, Brady TJ, Rosen BR. Functional mapping of the human visual cortex by magnetic resonance imaging. Science. 1991; 254:716–719. [PubMed: 1948051]

Boxerman JL, Hamberg LM, Rosen BR, Weisskoff RM. MR contrast due to intravascular magnetic susceptibility perturbations. Magnetic Resonance in Medicine. 1995; 34:555–566. [PubMed: 8524024]

Buxton RB, Wong EC, Frank LR. Dynamics of blood flow and oxygenation changes during brain activation: the balloon model. Magnetic Resonance in Medicine. 1998; 39:855–864. [PubMed: 9621908]

Duelli R, Kuschinsky W. Changes in brain capillary diameter during hypocapnia and hypercapnia. Journal of Cerebral Blood Flow and Metabolism. 1993; 13:1025–1028. [PubMed: 8408311]

Harel N, Lin J, Moeller S, Ugurbil K, Yacoub E. Combined imaging-histological study of cortical laminar specificity of fMRI signals. NeuroImage. 2006; 29:879–887. [PubMed: 16194614]

Kruger G, Glover GH. Physiological noise in oxygenation-sensitive magnetic resonance imaging. Magnetic Resonance in Medicine. 2001; 46:631–637. [PubMed: 11590638]

Leite FP, Tsao D, Vanduffel W, Fize D, Sasaki Y, Wald LL, Dale AM, Kwong KK, Orban GA, Rosen BR, Tootell RB, Mandeville JB. Repeated fMRI using iron oxide contrast agent in awake, behaving macaques at 3 Tesla. NeuroImage. 2002; 16:283–294. [PubMed: 12030817]

Lin AL, Fox PT, Yang Y, Lu H, Tan LH, Gao JH. Evaluation of MRI models in the measurement of CMRO2and its relationship with CBF. Magnetic Resonance in Medicine. 2008; 60:380–389. [PubMed: 18666102]

Lu H, Golay X, Pekar JJ, Van Zijl PC. Functional magnetic resonance imaging based on changes in vascular space occupancy. Magnetic Resonance in Medicine. 2003; 50:263–274. [PubMed: 12876702]

Lu H, Patel S, Luo F, Li SJ, Hillard CJ, Ward BD, Hyde JS. Spatial correlations of laminar BOLD and CBV responses to rat whisker stimulation with neuronal activity localized by Fos expression. Magnetic Resonance in Medicine. 2004; 52:1060–1068. [PubMed: 15508149]

Lu H, Scholl CA, Zuo Y, Stein EA, Yang Y. Quantifying the blood oxygenation level dependent effect in cerebral blood volume-weighted functional MRI at 9.4T. Magnetic Resonance in Medicine. 2007; 58:616–621. [PubMed: 17763339]

Malonek D, Grinvald A. Interactions between electrical activity and cortical microcirculation revealed by imaging spectroscopy: implications for functional brain mapping. Science. 1996; 272:551–554. [PubMed: 8614805]

Mandeville JB, Jenkins BG, Chen YC, Choi JK, Kim YR, Belen D, Liu C, Kosofsky BE, Marota JJ. Exogenous contrast agent improves sensitivity of gradient-echo functional magnetic resonance imaging at 9.4 T. Magnetic Resonance in Medicine. 2004; 52:1272–1281. [PubMed: 15562489]

Mandeville JB, Marota JJ, Kosofsky BE, Keltner JR, Weissleder R, Rosen BR, Weisskoff RM. Dynamic functional imaging of relative cerebral blood volume during rat forepaw stimulation. Magnetic Resonance in Medicine. 1998; 39:615–624. [PubMed: 9543424]

Ogawa S, Lee TM, Nayak AS, Glynn P. Oxygenation-sensitive contrast in magnetic resonance image of rodent brain at high magnetic fields. Magnetic Resonance in Medicine. 1990; 14:68–78. [PubMed: 2161986]

Ogawa S, Menon RS, Tank DW, Kim SG, Merkle H, Ellermann JM, Ugurbil K. Functional brain mapping by blood oxygenation level-dependent contrast magnetic resonance imaging. A comparison of signal characteristics with a biophysical model. Biophys J. 1993; 64:803–812. [PubMed: 8386018]

Triantafyllou C, Hoge RD, Krueger G, Wiggins CJ, Potthast A, Wiggins GC, Wald LL. Comparison of physiological noise at 1.5 T, 3 T and 7 T and optimization of fMRI acquisition parameters. NeuroImage. 2005; 26:243–250. [PubMed: 15862224]

Weinstein JS, Varallyay CG, Dosa E, Gahramanov S, Hamilton B, Rooney WD, Muldoon LL, Neuwelt EA. Superparamagnetic iron oxide nanoparticles: diagnostic magnetic resonance imaging and potential therapeutic applications in neurooncology and central nervous system inflammatory pathologies, a review. Journal of Cerebral Blood Flow and Metabolism. 2010; 30:15–35. [PubMed: 19756021]

Weisskoff RM, Zuo CS, Boxerman JL, Rosen BR. Microscopic susceptibility variation and transverse relaxation: theory and experiment. Magnetic Resonance in Medicine. 1994; 31:601–610. [PubMed: 8057812]

Yacoub E, Harel N, Ugurbil K. High-field fMRI unveils orientation columns in humans. Proceedings of the National Academy of Sciences of the United States of America. 2008; 105:10607–10612. [PubMed: 18641121]

Zhao F, Wang P, Hendrich K, Ugurbil K, Kim SG. Cortical layer-dependent BOLD and CBV responses measured by spin-echo and gradient-echo fMRI: insights into hemodynamic regulation. NeuroImage. 2006; 30:1149–1160. [PubMed: 16414284]

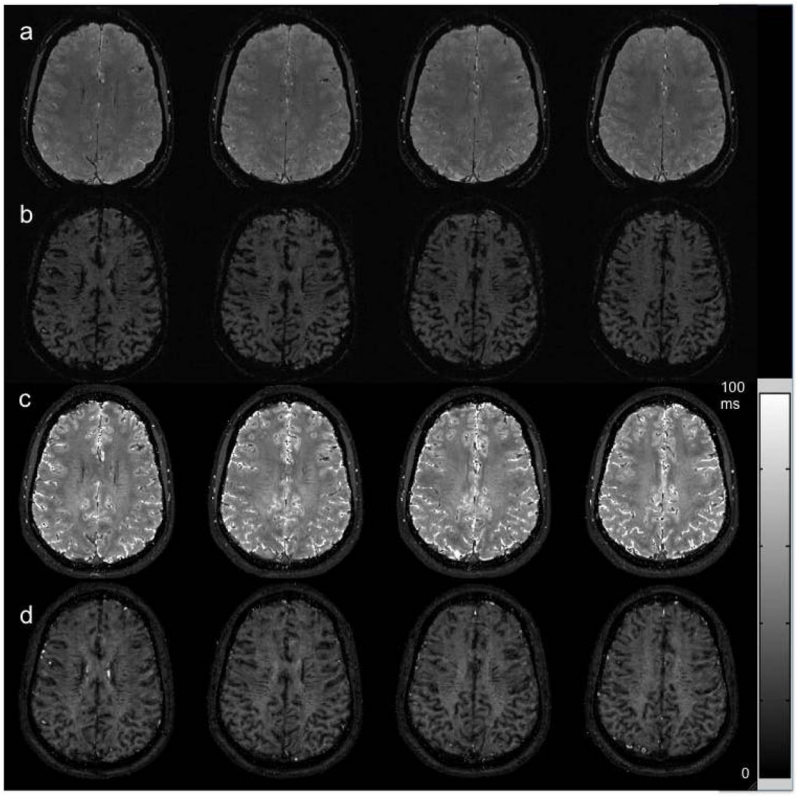

Figure 1.
T2*-weighted image at TE = 31.5ms (a) before and (b) after contrast injection, T2* map (c) before and (d) after contrast injection. The signal drops after contrast injection due to the strong T2* effect of USPIO, and the signal drop was larger in gray matter than in white matter, as CBV is higher in gray matter than white matter. See Table 1 for statistics of each subject.

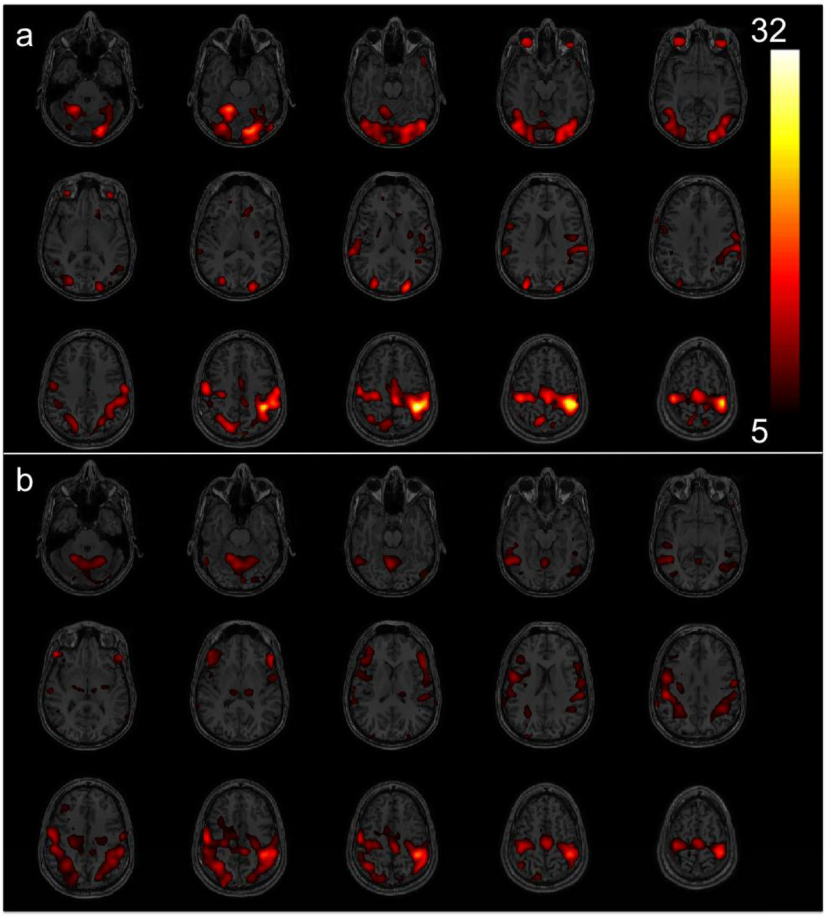

Figure 2.
Activation maps of CE-fBVI (a, top panel) and BOLD (b, bottom panel) respectively overlaid on T1-weighted anatomical images. Activation was observed for both BOLD and CE-fBVI, in regions including primary and supplemental motor regions, and the cerebellum. Discrepancy was also found in activated regions between the two methods. For example, a large activated region was found in the occipital cortex with CE-fBVI but not with BOLD. Higher student's t-statistics were found for CE-fBVI compared to BOLD.

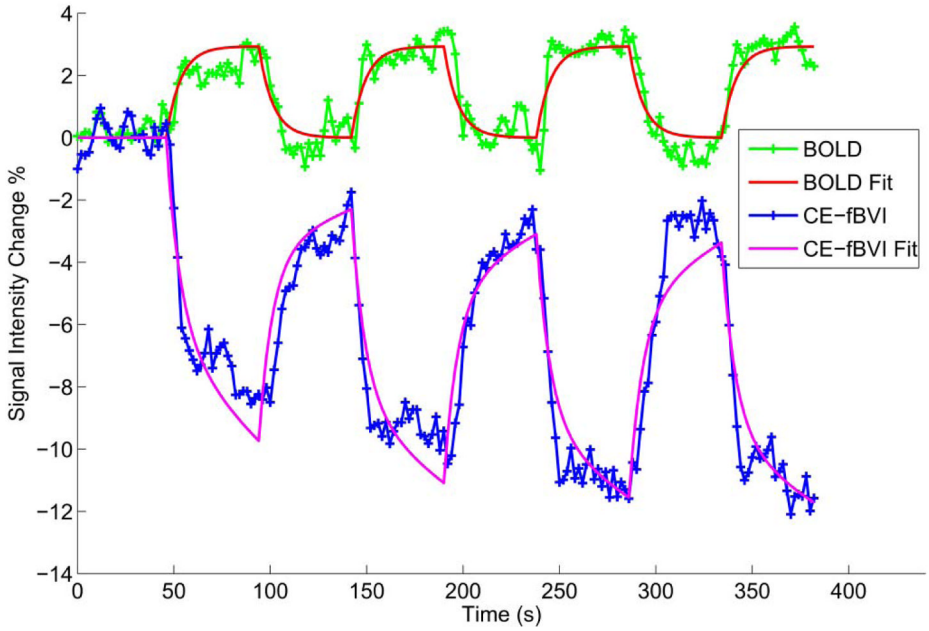

Figure 3.

An example of signal time course during BOLD (TE=35ms) and CE-fBVI (TE=20ms) acquisition in a 24-year-old right-handed male. The signal change was normalized to the base line value of BOLD to give a percentage signal change. The paradigm was four epoch of 48s of resting and 48s of finger tapping. The BOLD effect induces positive signal change, while CE-fBVI induces negative signal changes due to increases in CBV. The CE-fBVI response did not completely return to baseline after 48s of resting due to a slower component of response to stimuli. The contrast to noise ratio gain of CE-fBVI over BOLD was 2.9 in this subject.

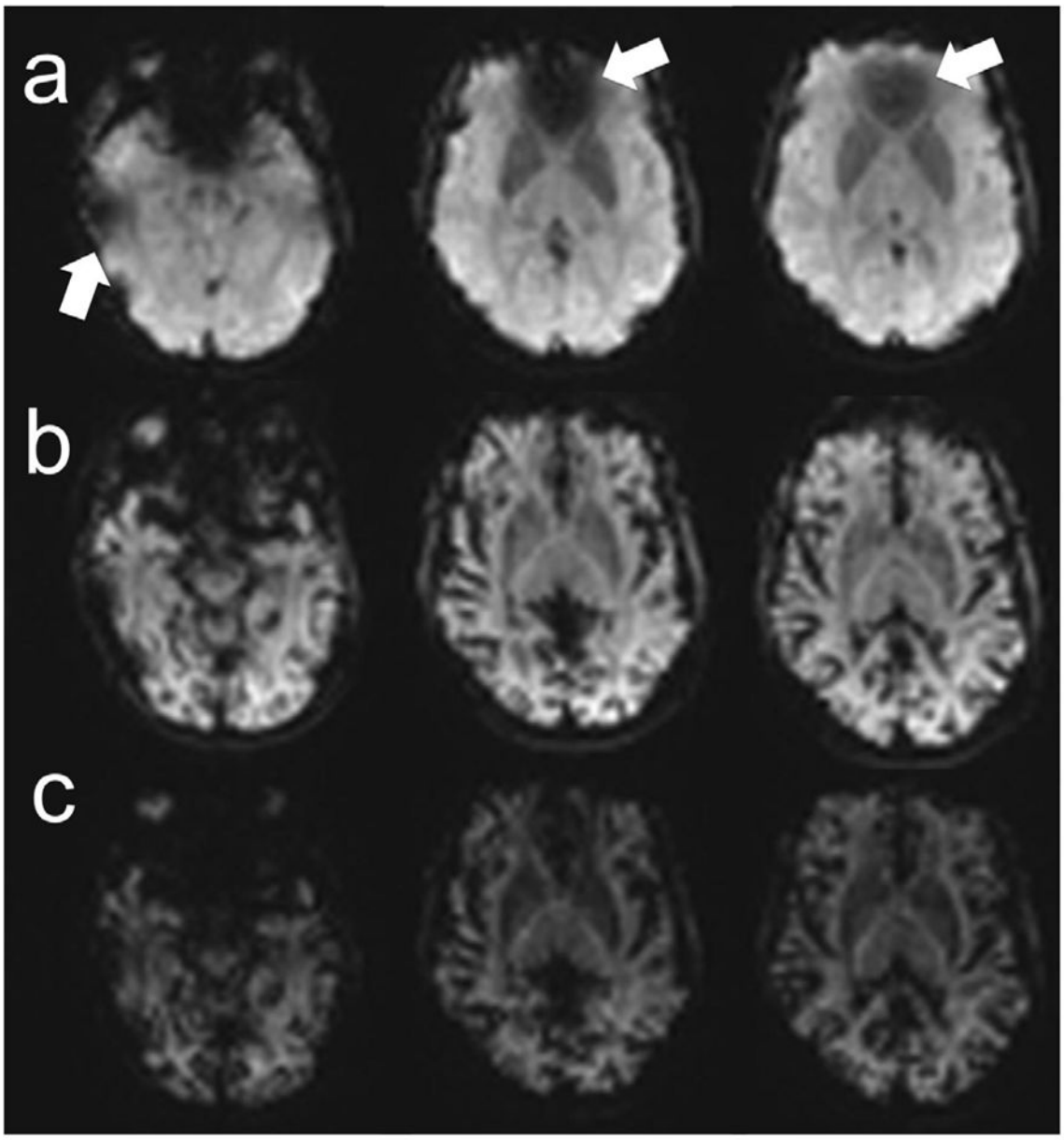

Figure 4.

T2* weighted EPI images with (a) BOLD at TE=35ms before contrast injection, (b) with CE-fBVI at TE=20ms after contrast injection and (c) with CE-fBVI at TE=35ms after contrast injection. The image intensity was scaled with the same window/level. Severe signal dropout was observed for BOLD images at the inferior frontal and temporal regions near air-tissue interface (arrows). The dropout was significantly alleviated with CE-fBVI at TE=20ms due to the use of shorter TE and the higher magnetic susceptibility value of USPIO. The alleviation of the dropout was smaller though also noticeable with CE-fBVI at TE=35ms.

Table 1

Mean and standard deviation of T2* value of the gray matter before and after contrast injection for each subject

Subject	T2* pre (ms)	T2* post (ms)
1	48.3 (12.5)	20.6 (8.0)
2	50.8 (8.4)	25.3 (9.4)
3	50.9 (9.1)	23.4 (6.7)
4	53.1(12.1)	23.5 (9.1)

Table 2

Time constants and weighting coefficients of BOLD and CE-fBVI signal response to stimuli

BOLD			CE-fBVI			
Subject	**Tc (s) (mono)**	**TE (ms)**	Tc_1 **(s)**	a_1	Tc_2 **(s)**	a_2
1	7.0	20	5.6	0.89	115.4	0.11
1	-	35	5.6	0.88	67.2	0.12
2	8.0	35	7.0	0.83	55.5	0.17
3	7.4	20	7.0	0.86	90.0	0.16
4	3.8	35	3.9	0.92	48.2	0.08

Table 3

Peak T (T_{peak}), average T value in the 50 most significant voxels in the primary motor cortex (T_{50}), average T value in regions commonly activated in both BOLD and CE-fBVI, the mean signal intensity of gray matter (S_{GM}) and temporal standard deviation of signal in gray matter (SD_{GM})

Subjects	Method	T_{peak}	T_{50}	T_{cn}	S_{GM}	SD_{GM}
TE=20ms for CE- fBVI	BOLD	18.6 (1.7)	14.6 (1.5)	7.9 (0.2)	3458.0 (144.2)	46.0 (4.3)
	CE-fBVI	29.0 (10.9)	23.2 (10.2)	8.6 (1.4)	2605.5 (26.1)	42.9 (2.6)
TE=35ms for CE- fBVI	BOLD	20.8 (7.0)	17.0 (0)	10.2 (5.0)	3501.3 (59.0)	38.2 (4.1)
	CE-fBVI	28.6 (8.4)	21.7 (7.0)	9.3 (1.0)	1222.3 (81.9)	34.4 (12.6)